Available online at www.sciencedirect.com

SciVerse ScienceDirect

Ceramics International 39 (2013) S533–S536

CERAMICS INTERNATIONAL

www.elsevier.com/locate/ceramint

Physical properties and bioactivity of nanocrystalline hydroxyapatite synthesized by a co-precipitation route

Suchittra Inthong, Tawee Tunkasiri*, Sukum Eitssayeam, Kamonpan Pengpat, Gobwute Rujijanagul

Department of Physics and Materials Science, Faculty of Science, Chiang Mai University, Chiang Mai 50200, Thailand

Available online 16 October 2012

Abstract

In the present work, the hydroxyapatite (HA) fine powders were synthesized through the co-precipitation in conjunction with ultrasonic vibration with various pH. The effects of solution pH on the formation and morphology of the HA powders were investigated. The obtained powders and sintered samples were characterized using various techniques. The bioactivity test was also examined by using stimulate body fluid (SBF). Pure HA was obtained without any calcination process. The formation and particle morphology of pure HA powders varied with the pH of the solution, changing from needle like to round shape as the pH increased from 5 to 11. The pH 11 ceramic sample exhibited high thermal stability, while pure phase HA was still present after sintering at 1300 °C. The pH level also affected the properties of the studied ceramics. The bioactivity test revealed that the pH 8 sample showed a higher amount apatite layer on the surface than the other samples.

Keywords: D. Apatite; E. Biomedical applications; Precipitation

1. Introduction

Hydroxyapatite [$Ca_{10}(PO_4)_6(OH)_2$; HA] is one of the most widely employed bioceramics since it can be used for human body part replacement. They can be used to replace bone and teeth because HA ceramics are inert to body fluids and have a high compressive strength. The HA may also be employed in the form of powders, porous blocks or beads to fill bone defects or voids. These defects may arise when large sections of bone have been removed (e.g., bone cancers) or when bone augmentations are required (e.g., maxillofacial reconstructions or dental applications) [1]. Recently, HA materials have been applied to drug delivery systems including the delivery of anti-tumor agents and antibodies for the treatment of osteomyelilis [2]. Synthetic hydroxyapatite has also been widely used for repairing hard tissues due to its chemical and structural similarity to the mineral phase of bone and tooth. Different clinical applications of hydroxyapatite involve the repair of bone defects, bone augmentation, as well as coatings for human body metallic implants [3]. Several different HA synthesis techniques have been developed in recent years such as direct precipitation from aqueous solutions [4], sol–gel procedures [5] and hydrothermal synthesis [6]. The generation of homogeneous and high purity nano-size powders is one of the main objectives of HA preparation. The control of the pH of the solution was found to be an important parameter for the synthesis of the HA powders [7]. In this work we present a preparation of HA nano-powders created using the co-precipitation method in conjunction with ultrasonics. The reason why this technique was used, is less time consuming synthesis and cheaper expense for processing. The effect of varying the pH of the solution was studied. Properties of ceramics prepared from the synthesized powder were investigated.

2. Experimental

The HA powders were prepared using the co-precipitation technique. Initially the diammonium hydrogen phosphate solution was slowly dropped into a calcium nitrate solution.

*Corresponding author. Tel.: +6653943376; fax: +6653357512.
E-mail address: tawee.tun@cmu.ac.th (T. Tunkasiri).

0272-8842/$ - see front matter © 2012 Elsevier Ltd and Techna Group S.r.l. All rights reserved.
http://dx.doi.org/10.1016/j.ceramint.2012.10.129

The pH of the mixture was then varied from 4 to 11, by adding the ammonium hydroxide solution. The ultrasonic finger was put into the solution and the temperature of the solution was maintained at 48 °C throughout the precipitation process. After completion of the reaction, the slurry was formed in the solution. It was separated by filtration and thoroughly washed with deionized water to remove the NO^{3-} and NH^{4+} ions before a final wash with ethanol.

The obtained powders were dried and pressed into discs of 15 mm in diameter and 2 mm in thickness using the uniaxial pressing technique. Then the green discs were sintered at 1300 °C for 2 h under normal air atmosphere. The densities of all ceramics were determined after sintering using the Archimedes method. The phase purity and crystal structure of the obtained powders were examined by X-ray diffraction technique (XRD, Rigaku Mini Flex II) with Cu-K_α radiation (λ) 1.5406 (Å), employing a scanning rate of 0.020 s^{-1} in the 2θ range from 20° to 60°. The morphology of the HA nanoparticles and ceramic surfaces were examined by scanning electron microscope (SEM, JEOL JSM-6335F) using a field emission SEM (FE-SEM). For mechanical examination, the Vickers hardness test was performed on the polished surface of the samples using a microhardness tester. For biological testing, the obtained ceramics were soaked into a simulated body fluid (SBF) at 37 °C for 14 days. Morphology of the soaked samples was examined by SEM.

3. Result and discussion

The XRD patterns of precipitated powders prepared at different pH are displayed in Fig. 1. The diffractograms revealed that all samples except the pH=4 sample showed pure HA phase. The analysis was carried out based on the JCPDS 09-0432. It should be noted that precipitation through the ultrasonic process can produced pure HA powder without any calcinations process. In addition, the XRD peak positions of all samples remained unchange, suggesting that the lattice parameters of the precipitated HA powder remained the same. Further, the XRD peaks exhibit a low intensity, indicating that the samples had low degree of crystallinity. To check the effect of pH on the degree of crystallinity (X_c) [8], the X_c was estimated using the expression

$$B_{0\ 0\ 2}\sqrt[3]{X_c} = K \quad (1)$$

where $B_{0\,0\,2}$ is full width at half maximum (FWHM) of peak (0 0 2) plane XRD reflection and K is a constant (~0.24). In the inset of Fig. 1, it can be seen that there is no relation between X_c and pH, however the values of X_c indicated that the pH=7 samples exhibited the highest degree of crystallinity.

SEM images of the synthesized powders are displayed in Fig. 2. All powders exhibited a very fine grain structure (nano-particles) and pH had an effect on particle morphology. Further, the powder exhibited higher agglomeration with increased pH levels. For the pH 5 sample, the particles of obtained powder showed a plate like shape Fig. 2(a). The average thickness of the plate was 20 nm and 500 nm in average length. The shape of particles became rounded with increasing pH. For example, the pH 7 sample had about 300 nm long spikes (Fig. 2(b)) while the pH 11 sample showed rather round grain with the average diameter of 100 nm (Fig. 2(c)).

Fig. 3 shows XRD patterns of sintered pellets prepared with different pH levels. The main phase of the sintered pellets is HA, but second phase such as α-tricalcium phosphate still occurred for most samples. However, it should be noted that pure phase of HA was present for the pH 11 samples, while previous works reported that the second phase only occurred at lower sintering temperature ($\leq$1150 °C). The same results were also obtained by Mostafa [9] and Raksujarit et al. [10]. This result indicates that the pH affected the phase of the prepared samples.

Selected SEM images of fracture surface of the ceramics are displayed in Fig. 4. The porosity levels in the SEM images of fracture surfaces are consistent with the trend in measured density values (Table 1). The micro structural analysis also showed that change in pH resulted in a change in grain size. Average values of grain size, as calculated by the linear intercept method, were in a range of ~1.6–6.8 μm, but the pH 9 samples showed the highest value of 6.8 μm (Table 1).

It is known that mechanical hardness property is important for biomaterial applications. In the present work, the Vickers hardness test was chosen for the hardness examination. The Vickers hardness value as a function pH is listed in Table 1. It seems that there is no direction trend between pH and hardness value, but the pH 9 sample showed the maximum Vickers hardness value of 6.1 GPa. The higher hardness values of the samples could be linked to the density data where the high density was found for pH 9–11 samples.

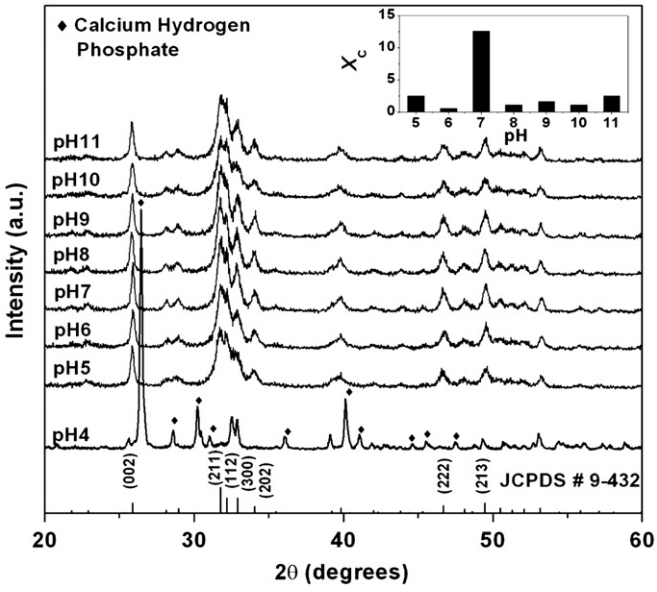

Fig. 1. X-ray diffraction pattern of as-dried HA. Inset shows degree of crystallinity of HA at various pH values.

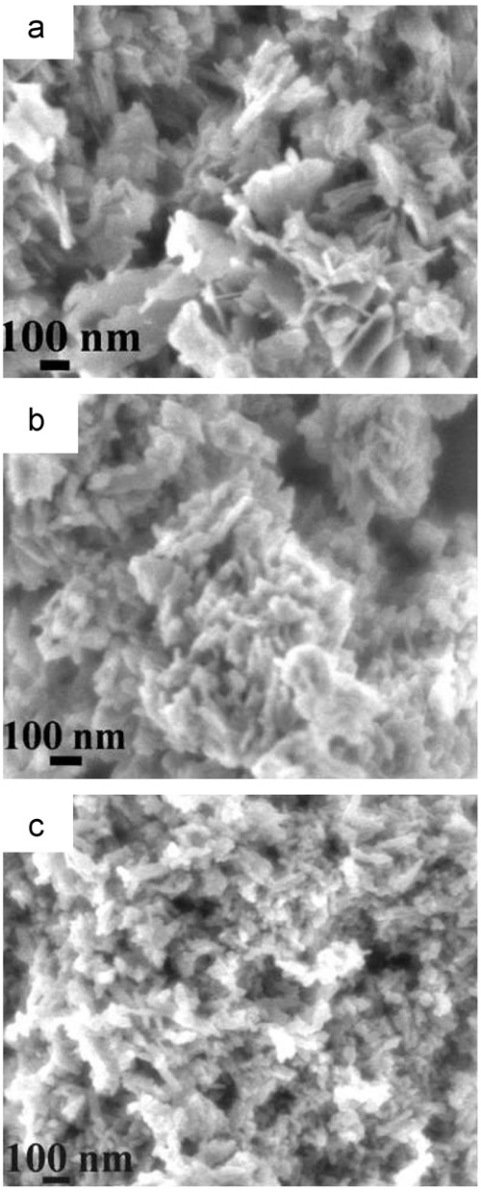

Fig. 2. Selected SEM images of hydroxyapatite powders prepared with different pHs: (a) pH 5, (b) pH 7, (c) pH 11.

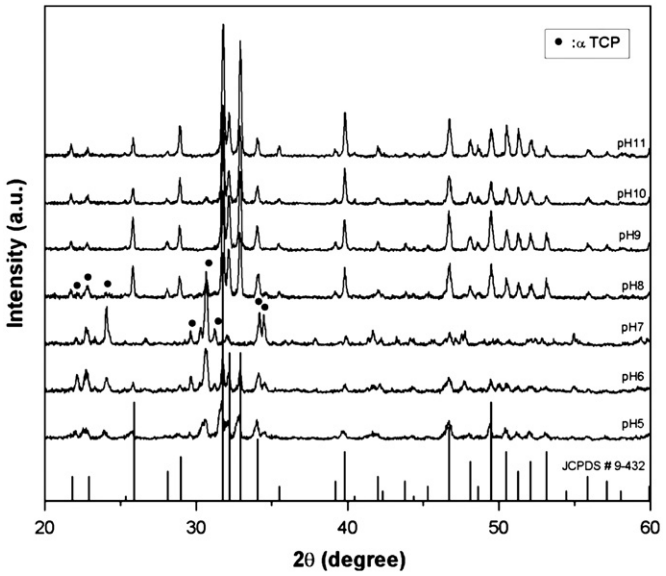

Fig. 3. X-ray diffraction pattern of the sintered pellets prepared with different pH levels and sintered at 1300 °C (●=α-tricalcium phosphate).

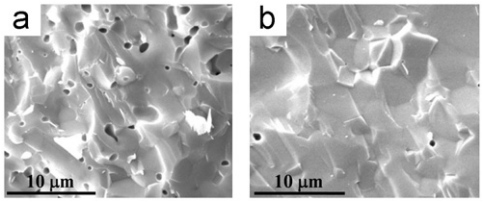

Fig. 4. SEM images of fracture surface for the ceramics prepared at: (a) pH 5 and (b) pH 11.

Table 1
Properties of HA ceramics prepared with different pH levels.

pH	Density (g/cm^3)	Grain size (μm)	Hardness (GPa)
5	2.75 ± 0.10	2.19 ± 0.74	3.12 ± 0.28
6	2.82 ± 0.14	1.64 ± 0.66	3.39 ± 0.29
7	2.83 ± 0.14	1.72 ± 0.81	3.50 ± 0.30
8	3.00 ± 0.10	5.97 ± 1.52	4.63 ± 0.24
9	3.04 ± 0.08	6.81 ± 1.48	6.06 ± 0.25
10	2.98 ± 0.15	4.34 ± 1.26	4.68 ± 0.23
11	3.02 ± 0.12	2.38 ± 1.06	4.67 ± 0.21

For bioactivity test the samples were immersed in SBF at 37 °C for 14 days. Tiny flakes or apatite layer were observed on the surface of all the tested samples (Fig. 5). This microstructure is similar to that observed in previous works [11]. However, the pH 8 sample showed higher amount of the flake structure (Fig. 5(b)). The Ca/P value has been determined by EDS at many areas of surfaces and it was in a range of 1.46–1.78. These values suggested a variation of apatite composition at the surface of the tested samples.

4. Conclusions

This work demonstrated that the co-precipitation method when associated with ultrasonic vibration could produce pure homogeneous and fine hydroxyapatite particles. The formation and morphology of the particles were found to depend on the pH (from 4 to11) of the solution. The particles changed from plate like to round shapes with increases in pH level. However, the pH ≤ 4 samples showed impure phase while the pH 7 sample had the highest crystallinity. Properties of ceramic samples prepared from the obtained powder were found to have no direction trend with the pH level. However, the pH 9 sample exhibited higher hardness value. In addition, the pH 8 samples showed a good response for the bioactivity testing.

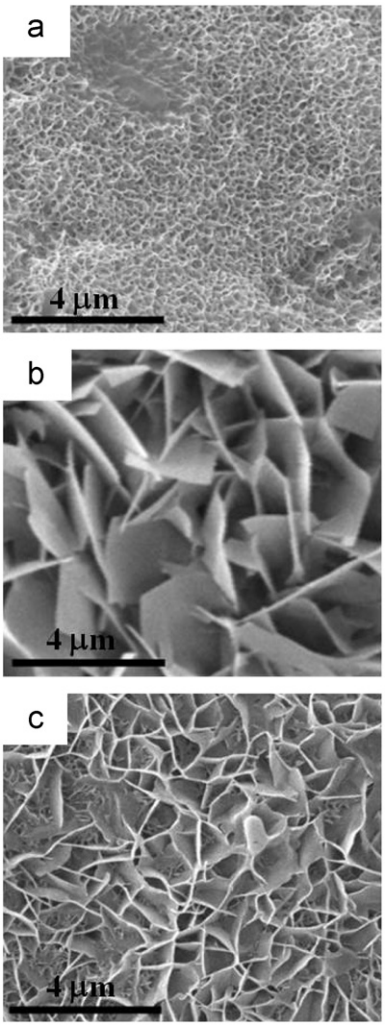

Fig. 5. Microstructure of the samples soaked in SBF solution: (a) pH 5, (b) pH 8, and (c) pH 11.

Acknowledgments

This work was supported by National Research University (NRU), Office of Higher Education Commission (OHEC), the Faculty of Science and the Graduate School of Chiang Mai University.

References

[1] J.B. Park, J.D. Bronzino, Metallic Biomaterials: Biomaterials Principles and Applications, Washington D.C., 2003.
[2] Y. Li, W. Tjandra, K.C. Tam, Synthesis and characterization of nanoporous hydroxyapatite using cationic surfactants as templates, Materials Research Bulletin 43 (2008) 2318–2326.
[3] L.L. Hench, J. Wilson, Hydroxyapatite coating an introduction to bioceramics, World Scientific, Singapore, 1993.
[4] I. Mobasherpour, M. Soulati Heshajin, A. Kazemzadeh, M. Zakeri, Synthesis of nanocrystalline hydroxyapatite by using precipitation method, Journal of Alloys and Compounds 430 (2007) 330–333.
[5] S.K. Padmanabhana, A. Balakrishnana, M.C. Chu, Y.J. Lee, T.N. Kim, S.J. Cho, Sol–gel synthesis and characterization of hydroxyapatite nanorod, Particuology 7 (2009) 466–470.
[6] X. Guo, P. Xiao, Effects of solvents on properties of nanocrystalline hydroxyapatite produced from hydrothermal process, Journal of the European Ceramic Society 26 (2006) 3383–3391.
[7] D.M. Liu, T. Troczynski, W.J. Tseng, Water-based sol–gel synthesis of hydroxyapatite: process development, Biomatters 22 (2001) 1721.
[8] A. Bianco, I. Cacciotti, M. Lombardi, L. Montanaro, E. Bemporad, M. Sebastiani, F-substituted hydroxyapatite nanopowders: thermal stability, sintering behaviour and mechanical properties, Ceramics International 36 (2010) 313–322.
[9] N.Y. Mostafa, Characterization thermal stability and sintering of hydroxyapatite powders prepared by different routes, Materials Chemistry and Physics 94 (2005) 333–341.
[10] A. Raksujarit, K. Pengpat, G. Rujijanagu, T. Tunkasiri, Processing and properties of nanoporous hydroxyapatite, ceramics, Materials and Design 31 (2010) 1658–1660.
[11] T. Kokubo, H. Takadama, How useful is SBF in predicting in vivo bone bioactivity, Biomatters 27 (2006) 2907–2915.